TISSUE ENGINEERING: Part A
Volume 15, Number 7, 2009

DOI: 10.1089/ten.tea.2008.0287

Characterization of Engineered Tissue Development Under Biaxial Stretch Using Nonlinear Optical Microscopy

Jin-Jia Hu, Ph.D.,* Jay D. Humphrey, Ph.D., and Alvin T. Yeh, Ph.D.

Little is known about the precise mechanical stimuli that cells sense and respond to as they maintain or refashion the extracellular matrix in multiaxially loaded native or bioengineered tissues. Such information would benefit many areas of research involving soft tissues, including tissue morphogenesis, wound healing, and tissue engineering. A custom tissue culture device has been constructed that can impart well-defined biaxial stretches on cruciform-shaped, fibroblast-seeded collagen gels and be mounted on the stage of a nonlinear optical microscopy (NLOM) system for microscopic characterization of matrix organization. The cruciform geometry permitted direct comparison of matrix (re-)organization within regions of the collagen gel exposed to either uniaxial or biaxial boundary conditions and examination by NLOM for up to 6 days. In addition, sequential NLOM measurements of collagen fiber orientations within gels while stretched, unloaded, or decellularized delineated contributions of applied stretches, cell-mediated tractions, and matrix remodeling on the measured distributions. The integration of intravital NLOM with novel bioreactors enables visualization of dynamic tissue properties in culture.

Introduction

The extracellular matrix provides vital structural integrity for many tissues and organs and plays equally important biological roles by influencing cell migration, proliferation, differentiation, and apoptosis. Among the many types of cells within the extracellular matrix, fibroblasts play a particularly important role by producing, maintaining, reorganizing, and degrading components of the matrix during normal development, tissue maintenance, adaptation, disease progression, and wound healing. Fibroblast-seeded collagen gels have thus been used as model systems to study cell–matrix interactions in tissue morphogenesis and wound healing.[1–3] In particular, the property of directed collagen contraction in uniaxially constrained, rectangular, fibroblast-seeded collagen gels has been used to engineer tissues with structural anisotropy.[4–6] Yet, contraction of the gel by embedded cells is not always desired; it can preclude control of the geometry and dimension of the construct and limit manipulation of its microstructure, which is important for ensuring normal functions.

Data collected over the past four decades reveal that fibroblast-mediated control of the matrix, and in particular the fibrillar collagens therein, is governed by both chemical and mechanical stimuli, with the mechanical loading often being multiaxial in many tissues. Nevertheless, little is known about the precise mechanical stimuli that fibroblasts sense and respond to as they refashion, replace, or remove collagen within multiaxially loaded native or bioengineered tissues. Without such understanding, we will neither be able to understand many natural processes, including tissue adaptations, disease progression, or wound healing, nor will we be able to engineer optimal tissue equivalents for restorative or regenerative medicine.

An emerging theme in fibroblast biology is that these cells seek to maintain nearly constant the stress within the matrix, a phenomenon that has been called tensional homeostasis.[7–11] For example, fibroblasts appear to establish a preferred endogenous tension when introduced into otherwise unstressed collagen gels; indeed, it appears that this tension is essential for cell survival. Tensional homeostasis is often associated with realignment or remodeling of the collagen fibers, yet much remains unknown with regard to effects due to imposed mechanical stretches or boundary conditions, roles of cell generated tractions, and cellular production or removal of fibers.

In this paper, we show an ability to combine nonlinear optical microscopy (NLOM) with a custom biaxial tissue culture device to study microstructural responses of fibroblast-seeded collagen gels to diverse static mechanical stretches during culture. Both NLOM and confocal reflectance microscopy have been used to characterize the organization of collagen within cell-free gels.[12,13] Confocal reflectance microscopy is similarly nondestructive for longitudinal studies

Department of Biomedical Engineering, Texas A&M University, College Station, Texas.
*Currently: Department of Mechanical Engineering, National Chiao Tung University, Hsinchu, Taiwan, Republic of China.

over time and sensitive to matrix morphology, but its lack of chemical specificity can complicate interpretation of multicomponent constructs.[14–17] Other optical techniques, for example, small-angle light scattering (SALS),[18,19] elastic scattering spectroscopy,[20] and polarized light microscopy,[21] have also been used to monitor matrix fiber orientation during mechanical loading or stimulation of tissues and constructs. Transmissive optical techniques are limited by the optical properties of tissue to thin or processed specimens. In particular, hyperosmotic agents have been employed with SALS to reversibly clear turbid tissues even though these agents can destabilize high order collagen structures.[22,23] Recently, Tan *et al.*[24] combined NLOM with optical coherence microscopy and demonstrated its capability in noninvasive imaging of cellular activities in three dimensions. Herein, however, we exploit the ability of NLOM to quantify collagen fiber orientations within a single gel, while it is subjected to different mechanical stretches or sequential treatments. Without fixation and processing, which can introduce artifacts if not performed properly (e.g., incomplete fixation of some constituents of the specimen), NLOM provided new insight into separate contributions of applied stretches, cell-mediated traction fields, and matrix remodeling to observed collagen fiber realignment in culture. For example, we found that equibiaxial and nonequibiaxial constraints, which imposed different boundary conditions on cell-mediated traction, can maintain the size and shape of a gel while simultaneously influencing microstructural anisotropy and thus can be used to help engineer collagenous tissues with controlled matrix organization.

Materials and Methods

Cell-seeded collagen gel preparation

3T3 cells (ATCC) were maintained in culture in Dulbecco's modified Eagle's medium (Invitrogen, Carlsbad, CA), containing 10% calf serum and antibiotics, and passaged every 6–7 days. Confluent cells between passages 5 and 7 were detached by 0.05% trypsin-ethylenediaminetetraacetic acid (Invitrogen), counted, and resuspended in culture medium at 1.15×10^6 cells/mL to be incorporated into collagen gels. Cell-seeded collagen gels were prepared on ice to avoid premature gelation. Specifically, 0.45 mL of reconstituted buffer (10×) was mixed with 0.9 mL of Dulbecco's modified Eagle's medium solution (5×) and 1.2 mL of concentrated collagen type I (9.37 mg/mL; BD Biosciences, San Jose, CA), mixed thoroughly, and then neutralized by ~110 μL of 0.1 N sodium hydroxide before adding 1.95 mL of the cell suspension. The final densities of cells and collagen were thus 5×10^5 cells/mL and 2.5 mg/mL, respectively. This mixture was poured into a cruciform mold (50 mm in length with each arm 15 mm in width at the end but tapered to 7 mm at the center) consisting of a silicone gasket placed within a 150×20 (diameter×height, mm) glass Petri dish. Porous polyethylene bars (Small Parts, Miramar, FL) were positioned at each end of the four arms of the mold before adding the collagen–cell mixture. Cell-seeded collagen gels were formed in the mold at 37°C in a humidified CO_2 incubator. The silicone gasket was removed after 30 min of gelation, and the collagen gel was cultured in 40 mL of culture media within an incubator for an additional 24 h before coupling to the biaxial tissue culture device.

Biaxial tissue culture device and culturing conditions

A custom biaxial tissue culture device was built to impart well-defined biaxial stretches to a cruciform-shaped (cell-seeded collagen) gel and to be mounted on the microscope stage of the NLOM system for intravital imaging.[25] Briefly, the device is made of polycarbonate and stainless steel and can be autoclaved for sterilization. Cruciform-shaped, fibroblast-seeded collagen gels were clamped within the device via embedded porous polyethylene bars at each end of the four arms and stretched to a prescribed extent (Figs. 1A and 2): 1.01×1.01 equibiaxial stretch; 1.01×1.1, 1.01×1.2, and 1.1×1.2 strip biaxial stretch; or 1.2×1.2 equibiaxial stretch. Three stretch states (1.01×1.01, 1.01×1.2, and 1.2×1.2) were characterized by NLOM over time. For these time studies, the chamber was placed in a 37°C humidified CO_2 incubator except when imaged by NLOM. For gels under 1.01×1.2 strip biaxial stretch, three regions of the gel, which experienced three different stretch states, were imaged (Fig. 1B): central (CT), long arm (LA), and short arm (SA). The

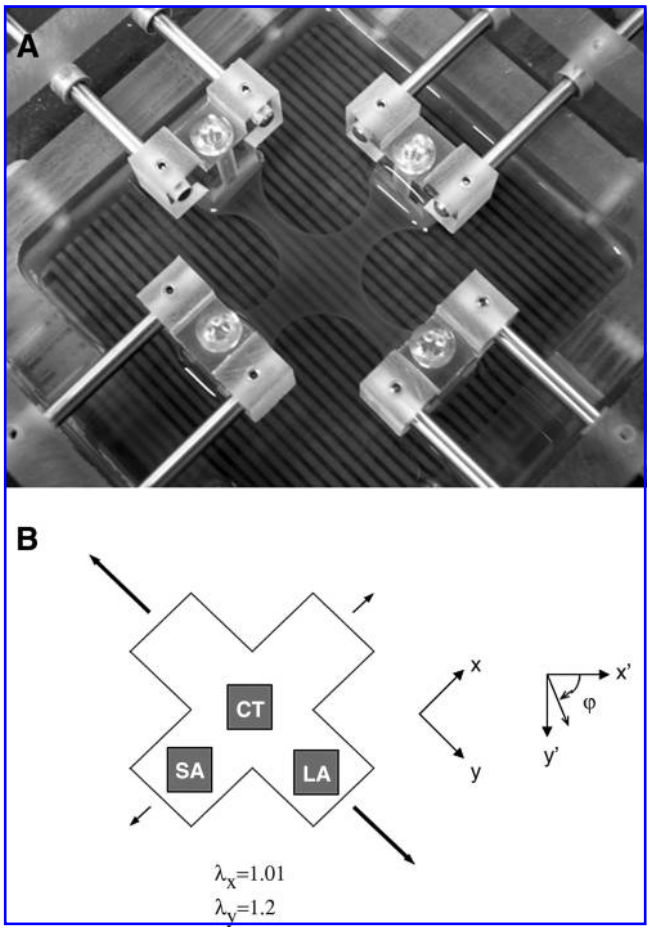

FIG. 1. Photograph of a cruciform-shaped collagen gel clamped within the biaxial culture chamber and subjected to a strip biaxial stretch (**A**). Schematic diagram of the strip biaxial stretched gel (**B**). NLOM images were acquired from the shaded regions, that is, central (CT), long arm (LA), and short arm (SA). The coordinate systems used for stretching mechanics (x, y) and NLOM imaging (x', y') were oriented at $\varphi = \sim 45^\circ$ relative to each other.

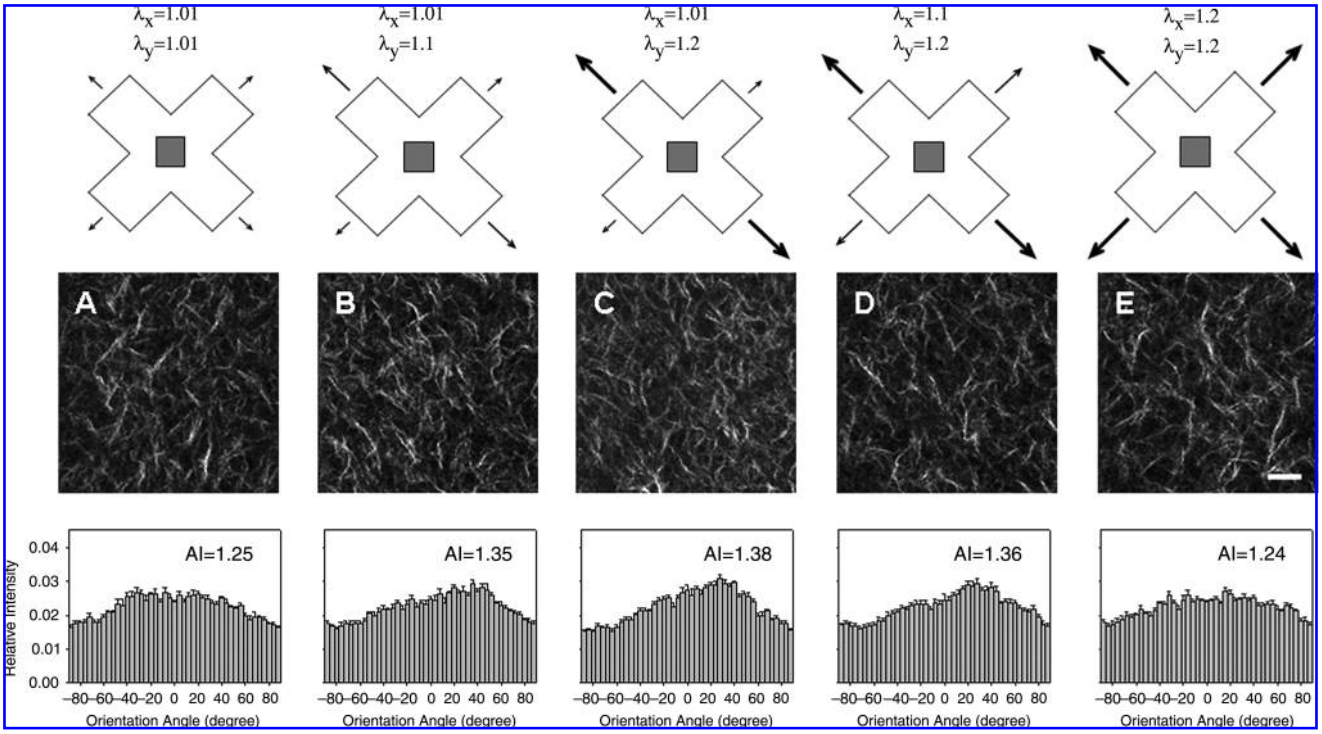

FIG. 2. (Top) Schematic of stretching protocols, with λ, the global stretch ratio. Images were acquired from the shaded region. (Middle) Representative NLOM images of fibrillar collagen using SHG for biaxial stretches (λ_x, λ_y) of (1.01, 1.01) (**A**), (1.01, 1.1) (**B**), (1.01, 1.2) (**C**), (1.1, 1.2) (**D**), and (1.2, 1.2) (**E**). Scale bar represents 20 μm. (Bottom) Collagen fiber distribution and alignment indices (AIs). Error bars are standard errors ($n = 5$ images each).

axes for stretch (x–y) and NLOM imaging (x'–y') were oriented at $\varphi = \sim 45^\circ$ relative to each other as illustrated in Figure 1B. The distributions of collagen fiber orientation were examined on days 0, 3, and 6 under stretched and then unloaded (gel released from loading bars) conditions. To identify contributions of cell traction on fiber orientation, one gel from each cultured group (day 3 or 6) was further treated with distilled (hypotonic) water in the unloaded condition before image acquisition.

Nonlinear optical microscopy

Our custom-built NLOM system has been described previously.[26] Briefly, sub-10-fs pulses from a Ti:Al_2O_3 oscillator (Femtosource; Femtolasers, Cambridge, MA) pumped by an Nd:YVO4 solid-state laser (Verdi; Coherent, Santa Clara, CA) were coupled into the epifluorescence port of an upright microscope (Axioskop2 MAT; Carl Zeiss, Thonnwood, NY) via dual-axis galvanometer–driven mirrors (Model 6220; Cambridge Technology, Lexington, MA) mounted on an elevated breadboard. The beam was directed to the microscope objective by a short pass dichroic mirror (635dcspxruv3p; Chroma, Rockingham, VT). Nonlinear optical signals were collected by the 40× focusing objective (numerical aperture = 0.8) and directed to a custom-built dual channel detector mounted on one of the dual accessory ports of the binocular head. The detector unit houses two dichroic mirrors and bandpass filters (Chroma), focusing lenses (31 2321; Linos Photonics, Milford, MA), and a pair of photon-counting photomultiplier tubes (R7400P; Hamamatsu, Bridgewater, NJ). Appropriate long pass dichroic mirrors and bandpass filters were used for collagen second harmonic generation (SHG) (430dcxru and HQ405/40, respectively; Chroma) and cellular two-photon excited fluorescence detection (580dcxr and HQ480/40, respectively; Chroma). Because of the distinct spectral characteristics of signals generated from cellular regions and extracellular collagen fibers, the two components were imaged and segmented simultaneously. Each photomultiplier tube was connected to a preamplifier/discriminaminator (F-100T; Advanced Research Instruments, Golden, CO) that thresholds signal current and converts it to transistor-transistor logic pulses for photon counting. Image intensities were displayed in photon counts per second on a personal computer (Optiplex GX280; Dell, Round Rock, TX). Throughout this experiment, less than 30 mW of laser power was incident on the scanning mirrors.

Image processing and analysis

Three SHG image stacks were acquired from each region of interest within the cruciform-shaped, fibroblast-seeded collagen gels. Optical sections were acquired from nearly the entire full thickness, probing as deep as 150 μm. Images containing no cells were randomly chosen for analysis. Collagen fiber orientation was analyzed by a Matlab routine based on a fast Fourier transform (FFT) algorithm.[27] For enhanced frequency resolution, the image was padded with the mean gray level of the image, extending the size of the image from 256×256 to 512×512 pixels. To reduce edge discontinuities, a two-dimensional Hann window function was applied to the padded image, resulting in the windowed image that was analyzed using a two-dimensional FFT. High and low butter filters were applied to the power spectrum of the image to remove high and low frequency signals. These cut-off

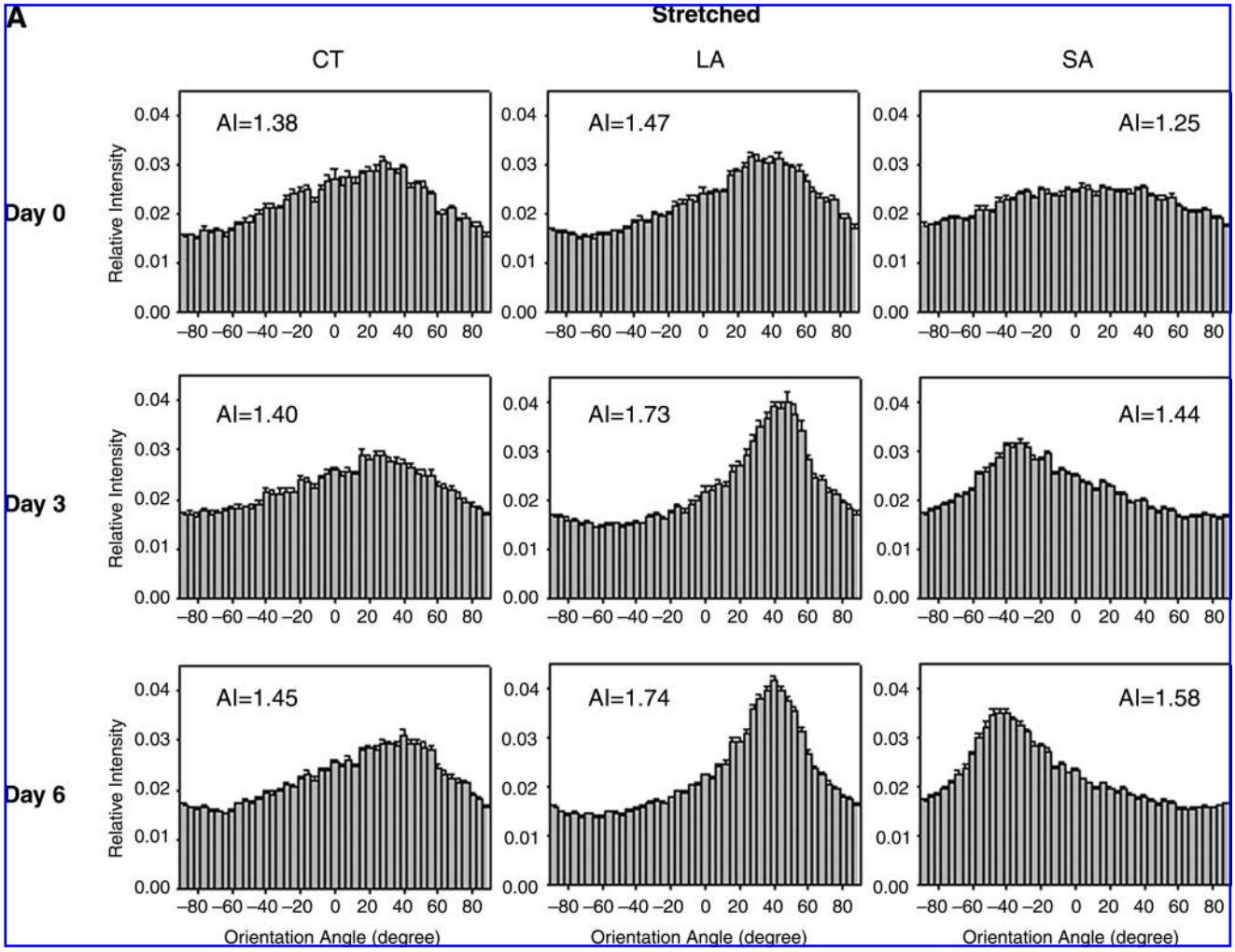

FIG. 3. Analyses of collagen fiber distributions for three regions (central, CT; long arm, LA; and short arm, SA) of strip biaxial stretched gels on days 0, 3, and 6 (**A**). NLOM images were acquired from gels while stretched. Normalized AI to day 0 in the three regions for days 3 and 6 (**B**). Error bars are standard errors. Significant differences ($p < 0.05$) are denoted by asterisks.

frequencies were selected based on outcomes of the inverse FFT of the filtered power spectrum image. The angular distribution was obtained by polar coordinate analysis of the filtered power spectrum image.[28] Briefly, the relative intensity (RT) for angles between Θ and $\Theta + 4^\circ$ was calculated by

$$RT(\Theta) = \sum_{\theta \geq \Theta}^{\theta < (\Theta+4)} g(r,\theta) \Big/ \sum_{\theta \geq 0}^{\theta < 180} g(r,\theta),$$

where $g(r, \theta)$ is the gray-scale level of a pixel at the polar coordinate in the filtered power spectrum image. An alignment index (AI) was then used to quantify distributions of collagen fiber orientations and to enable statistical comparisons among different treatments, that is, the fraction of collagen fibers lying within 20° of the predominant direction normalized by that of a random distribution (=0.22)[29]; values of AI range from 4.55 for strong alignment (i.e., parallel fibers) to 1.00 for random alignment.

Histology

After 3 or 6 days in culture, additional gels were fixed in 10% neutral-buffered formalin overnight in an unloaded condition. After standard processing, gels were embedded in wax, and 5 μm sections were cut and stained with H&E to examine cell orientations.

Statistical analysis

AIs were calculated for up to three regions of interest within a gel (see Fig. 1) based on five representative SHG images each. Differences between groups (e.g., days 0, 3, and 6, or sequential states) were assessed via one-way ANOVA with Holm–Sidak *post hoc* testing, with an overall significance level $p = 0.05$. Holm–Sidak testing is useful to correct for false-positives enumerated by the Bonferroni inequality and adequate for the relatively few number of comparisons in this study. Results are reported as mean ± standard error.

Results

SHG images of the CT region within a representative cruciform-shaped, fibroblast-seeded collagen gel at day 0 are shown in Figure 2 for five biaxial stretches (λ_x, λ_y): A (1.01, 1.01), B (1.01, 1.1), C (1.01, 1.2), D (1.1, 1.2), and E (1.2, 1.2); also shown are corresponding distributions of collagen fiber orientations and associated AIs (see Materials and Methods). The near-free floating condition (1.01, 1.01) shown in Figure 2A exhibited a fairly isotropic distribution of collagen fibers with AI = 1.25. Increased stretch along one axis to (1.01, 1.1) and then (1.01, 1.2) increased collagen fiber alignment toward the stretched direction (Fig. 2B, C), whereas subsequent stretch along the perpendicular axis to induce the (1.2, 1.2) equibiaxial condition (Fig. 2E) returned the fiber distribution toward that for the near-free floating condition observed in Figure 2A (AI = 1.25).

Collagen fiber orientations were compared across the three regions of interest (see Fig. 1B) over 6 days for the overall case of strip biaxial stretch (1.01, 1.2) as seen in Figure 3A. Whereas the CT region was subjected to strip biaxial stretch, the LA region was stretched uniaxially, and the SA region was merely anchored. On day 0, the fibers in the CT region tended to align toward the direction of 20% stretch; the fiber alignment was less dramatic compared to that in the LA region, however, as demonstrated by a smaller AI (1.38 vs. 1.47). Because the SA region was merely anchored (1% stretch), no specific fiber alignment was observed initially. On days 3 and 6, the collagen fiber orientations in the CT region were consistent with those observed on day 0 (see Fig. 2). Collagen fiber orientations in the LA and SA regions became more anisotropic by day 3, however. These time-dependent changes in alignment can be appreciated by normalizing the AI to the initial value (i.e., day 0) for each region. The normalized AI in the CT region was near unity over time, whereas it increased in the LA and SA regions by day 3 (Fig. 3B). Specifically, AI increased ~18% by day 3 and remained at a similar level on day 6 in the LA region (note that AI = 1.47 on day 0); AI increased ~15% by day 3 and ~25% by day 6 in the SA region (note that AI = 1.25 on day 0). Gels were maintained at their stretched states during imaging.

To help delineate the separate influences on fiber alignment by applied stretch, cell-mediated traction, and active remodeling of the matrix, gels were also imaged on days 3 and 6 while unloaded from the device and then with fibroblasts removed in the unloaded state (cell free). That is, contributions of applied stretch to fiber alignment (stretched) were excluded if images were acquired after the gel was released from the clamps (unloaded). Based on analyses of SHG images, we found that on day 0 any collagen fiber alignment induced by the applied stretch was reversed toward the original (isotropic, AI = 1.25) state as expected (data not shown). Upon release of stretched gels after 3 and 6 days in culture, there were different levels of randomization of collagen orientations relative to the corresponding stretched values. Unloaded AIs were significantly different from stretched AI except for the CT region for days 3 and 6 (Fig. 4B, D, respectively; see also Fig. 4A,C), with decreases in AIs smaller on day 6 than on day 3. Contributions by embedded fibroblasts were removed (cell free) by subjecting unloaded gels to hypotonic water; hence, associated fiber orientations were due solely to the developed anisotropy within the matrix. Removal of the cells caused statistically significant increases in AI relative to unloaded values in the CT and SA regions on day 3 (Fig. 4B), and thus evidence for anisotropic remodeling, but did not increase AI significantly in the LA region on days 3 and 6 (Fig. 4B, D). Recall that collagen fibers in the unloaded state were more aligned in the LA region compared with CT and SA regions (see Fig. 4). The distribution of fiber orientations in the SA region, in which applied stretch was negligible, tended to return to near stretched levels on days 3 and 6 (Fig. 4B, D). On day 6, sequential measurements of AI in the CT region under stretched, unloaded, and cell-free conditions were comparable (AI = 1.37, 1.33, and 1.32, respectively). Figure 5 shows representative NLOM images of the three sequential states (A, stretched; B, unloaded; and C, cell free) for the SA region of a 3-day gel. Of particular note was the alignment of collagen fibers, between two neighboring fibroblasts, perpendicular to the load axis in the unloaded state (Fig. 5B).

Histology provided a broader field of view than that of NLOM and thus was useful in mapping overall cell orientations, as, for example, in the unloaded state (Fig. 6). In the CT region, most cells tended to align in the stretched direction, but the alignment was less than that observed in LA or SA regions (Fig. 6A). Most cells in the LA region showed an elongated, bipolar shape, aligning in the direction of stretch (Fig. 6B). Most cells in the SA region appeared to align in the direction of constraint, but they were less elongated than those in the LA region (Fig. 6C). As a control, Figure 6D shows results from a freely floating gel; most cells exhibited a dendritic morphology, which has been reported as distinct from cells in gels under tension.[30]

Discussion

Collagen fibers can be aligned within tissues via at least four different mechanisms: a deformation-induced anisotropy that is reversible upon unloading, a cell traction–mediated alignment that relies on continued cell activity, establishment of chemical bonds within a stretched or contracted state that largely entrenches the alignment, and a cell-mediated deposition of new fibers at preferred orientations such as expected in cases of contact guidance. Without distinguishing between newly formed chemical bonds and new

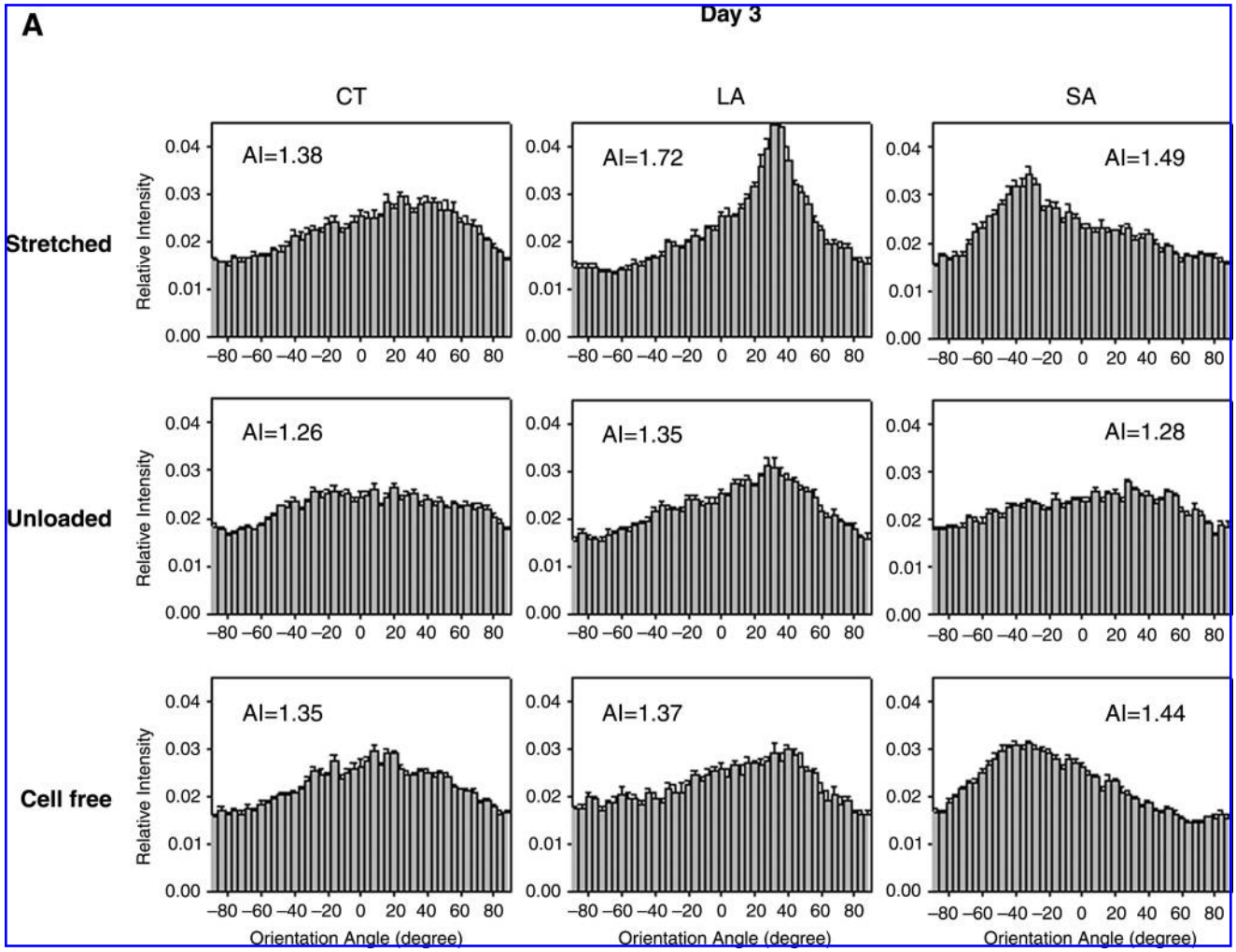

FIG. 4. Analyses of collagen fiber distributions and alignment indices (AIs) from three regions (central, CT; long arm, LA; and short arm, SA) of strip biaxial stretched gels while stretched, unloaded, and cell free at days 3 (**A, B**) and 6 (**C, D**). Error bars are standard errors. Significant differences ($p < 0.05$) are denoted by asterisks.

matrix deposition, these two mechanisms can be characterized as irreversible matrix growth and remodeling. Figure 2 shows that, as expected, different types of biaxial stretching induced marked changes in the alignment of collagen within the tissue equivalents. Whereas equibiaxial stretching (Fig. 2E) preserved alignments relative to the unstretched control (Fig. 2A), increasing the degree of preferential stretching in one direction (e.g., Fig. 2C) increased the alignment of the fibers within the CT region toward the direction of stretching. Indeed, given that the SA and LA of the cruciform-shaped sample (Figs. 1 and 3) provided further extremes in preferential stretching, it was not surprising that such

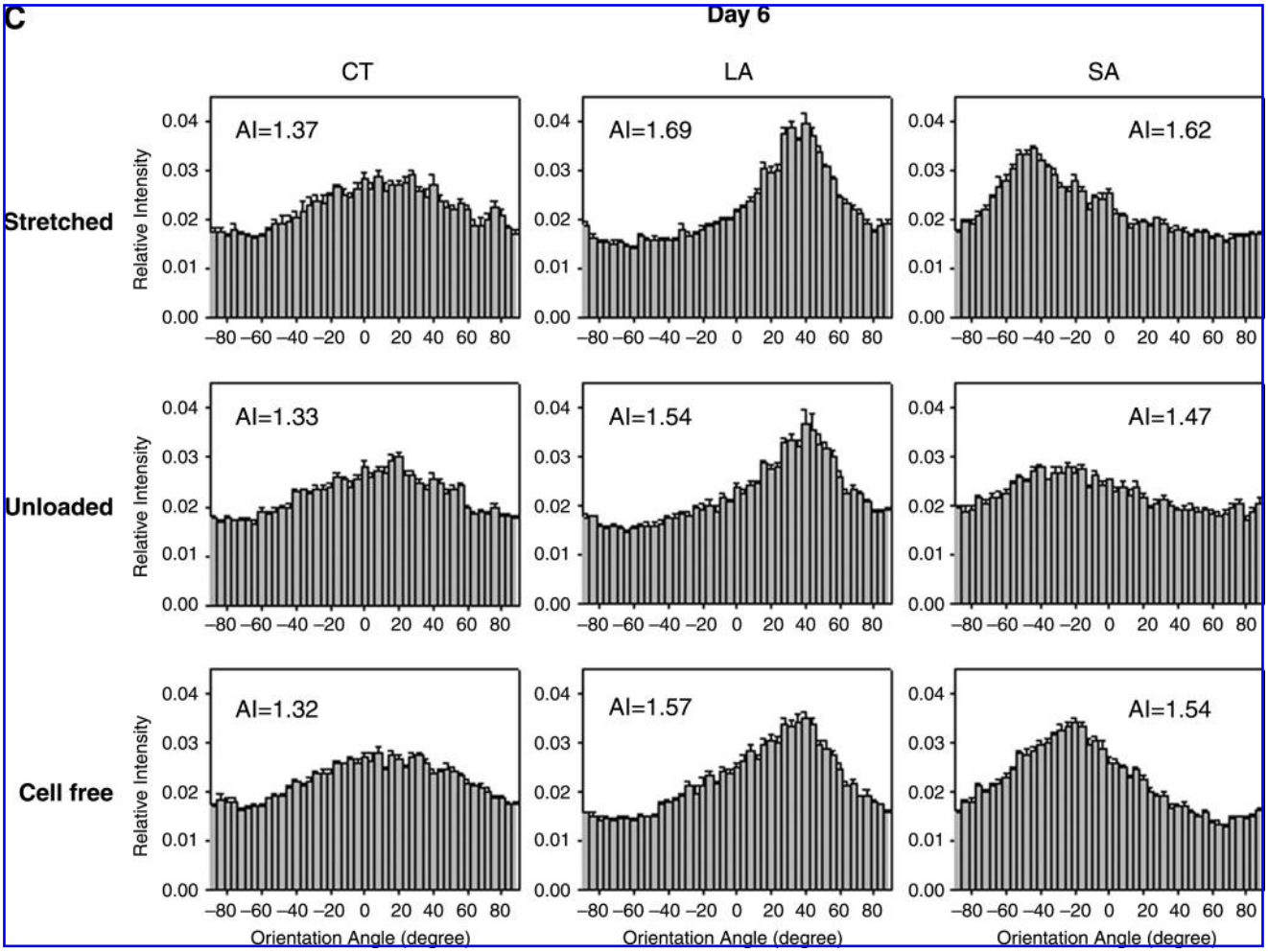

FIG. 4. (*continued*)

stretching was an effective way to align the fibers along the direction of stretch. We emphasize, however, that alignment was purposely measured within the middle of each of the three regions of the specimen studied (Fig. 1B), but was likely even greater near the free edges in the SA and LA.[21,31]

Collagen fiber alignment was observed to depend on both culture time (i.e., cell activity) and region (i.e., boundary conditions imposed by mechanical constraints). In the SA region, fiber alignment was induced gradually by the cell traction that developed between the two anchors. Following the same mechanism, the relatively weak fiber alignment established by the applied stretch at the onset of gel contraction was enhanced over time in the LA region. These aligned fibers may have provided environmental cues for the cells to reorient via contact guidance.[32,33] Although not directly examined in this study, aligned cells may synthesize collagen fibers with preferred orientations[34] and thereby contribute to overall changes in fiber orientation. In fact,

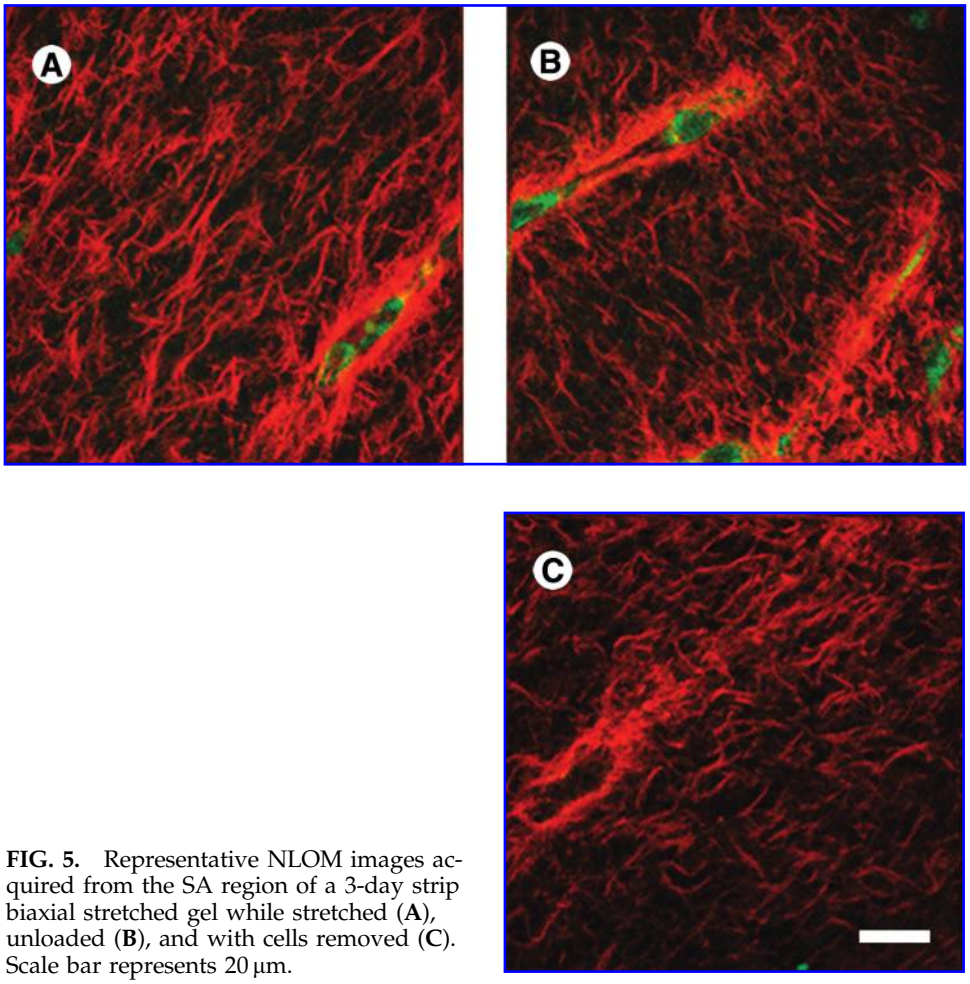

FIG. 5. Representative NLOM images acquired from the SA region of a 3-day strip biaxial stretched gel while stretched (**A**), unloaded (**B**), and with cells removed (**C**). Scale bar represents 20 μm.

interactive processes between cell and matrix have been shown in tissue remodeling (see Grinnell[11] for a review). In both LA and SA regions, in which lateral constraints were absent, alignment increased with duration of culture over 6 days (Fig. 3). This was consistent with the well-known directed collagen contraction in uniaxially constrained, rectangular fibroblast-seeded collagen gels.[4–6] Moreover, we found that in the CT region, collagen anisotropy remained consistent over 6 days of culture with that imposed initially, suggesting biaxial, as opposed to uniaxial, constraints may be used to prescribe tissue anisotropy with higher fidelity. Moreover, when gels were stretched equibiaxially (e.g., 20% stretch along both axes), collagen fibers distributed randomly in the CT region and did not develop further structural anisotropy over time (data not shown, see Thomopoulos *et al.*[16]). Although not shown, acellular gels did not increase in anisotropy in LA or SA regions over 6 days of culture, further implicating the important role of cell-mediated reorganization of the matrix.

Sequential measurements of collagen fiber orientations were performed, for the first time, on individual gels in stretched, unloaded, and cell-free states to isolate different mechanisms affecting matrix anisotropy. Upon release from the biaxial device, some randomization of collagen fiber orientations was generally observed at all days and in all regions. Subsequent measurements in unloaded, cell-free states showed a return in matrix anisotropy implicating fibroblast traction as a randomizing force. These observations were pronounced at day 3 (see Fig. 4). Indeed, collagen fibers were found to align perpendicular to the cell axis in unloaded gels at day 3 (see Fig. 5B). This suggests that tractions exerted by cells were not only localized at two polar ends but over the entire cell membrane. It is important to note that only when gels were unloaded was this phenomenon visible. The randomizing effect by the fibroblasts was less pronounced at day 6, however. Measured collagen fiber orientations of unloaded, cell-free gels showed persistent alignment, consistent with the accumulated effects of irreversible matrix remodeling, possibly including the establishment of chemical bonds that entrench alignment and/or matrix deposition at preferred orientations. The alignment of embedded cells revealed by histological sections from day 6 gels (fixed in unloaded state) supports such irreversible matrix remodeling. Indeed, entrenched alignment by irreversible matrix remodeling would be less susceptible to randomizing cell tractions.

If we use the measured distributions of collagen orientation within unloaded, cell-free gels as a metric of fibroblast-mediated matrix remodeling, the anisotropy observed on days 3 and 6 suggests that the rate of remodeling was the same in the LA and SA regions (Fig. 4). In other words, the rate of matrix remodeling was not different between regions

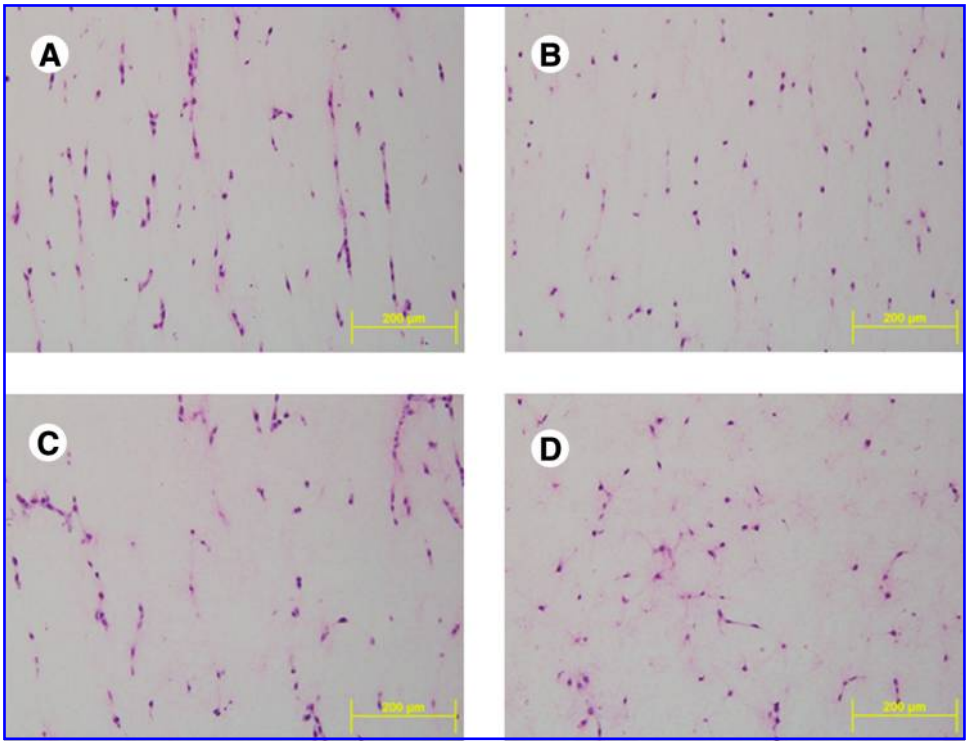

FIG. 6. Representative H&E-stained micrographs from the central (**A**), long arm (**B**), and short arm (**C**) regions of a 6-day strip biaxial stretched and from the central region (**D**) of a 6-day free floating gel. Color images available online at www.liebertonline.com/ten.

experiencing a step increase in stretch of 20% versus simple anchoring after 3 days. This was seen in Figure 4B and 4D, where cell-free AIs of the LA and SA regions were similar at each time point. Note, too, that at day 6 fiber alignment within the stretched state in the LA region appeared to be stronger than that in the SA region, thus suggesting a significant contribution by the applied stretch on fiber alignment.

Marenzana *et al.*[35] used scanning electron microscopy to show similarly significant alignment in uniaxially constrained collagen gels. Using a transducer to monitor directly the forces generated by fibroblast populated collagen gels over 60 h of culture, they showed that tension results from a combination of cell-mediated traction and a gradually increasing residual matrix tension. They suggested that this residual matrix tension, which accounted for ~50% of measured force after 60 h of culture, indicated "a time-dependent shortening of the collagen network, progressively stabilized into a built-in tension within the matrix." Although our results do not address possible shortening of the fibers, the entrenched realignment is consistent with the existence of a residual matrix tension that is presumably related to a tendency toward tensional homeostasis. A similar stable remodeling of collagen gels by fibroblasts was reported by Sawhney and Howard,[36] who emphasized the importance of fibroblast-generated traction fields in remodeling the matrix as reemphasized by Dahlmann-Noor *et al.*[37]

Finally, note that the measured AI necessarily provided an average over the field of view (~130×130 μm). It is expected that variations existed within such regions, particularly related to proximity of a collagen fiber to individual cells. Indeed, collagen fibers in a stretched gel tended to align parallel with dispersed cells (Fig. 5A), whereas they tended to align orthogonally between closely paired cells upon release of stretch (Fig. 5B). Feng *et al.*[38] similarly reported that "the orientation degree of the fibrils between two cells may be higher than that of fibrils in other locations related to the embedded cells," but this was not explored in detail. Increased intensity of SHG near the cells also suggested either an increased compaction of extant fibers[39] or an increased synthesis of new fibers by the cells.[40] Indeed, Kessler *et al.*[40] reported significant changes in gene expression within only 24 h in fibroblasts cultured within collagen gels or on flexible membranes. The altered gene expression profile suggested a phenotypic shift toward more synthesis of matrix (e.g., up-regulation of genes for α1[I], α2[I], and α1[III] collagen, and fibronectin) and decreased removal of matrix (e.g., down-regulation of matrix metalloproteinase (MMP-1) and up-regulation of tissue inhibitor of metalloproteinase (TIMP-1) and TIMP-3). We did not assess changes in gene expression or collagen production, however.

In this study, cell seeding density and initial collagen concentration were chosen to prevent overwhelming gel contraction, which can occur in hours, and were comparable to values used by others.[15,41,42] In addition to initial cell seeding density and collagen concentration, characteristics of embedded cells[43] and active components in the media[44,45] also affect the kinetics of collagen contraction. Fortunately, the cruciform shape of the cell-seeded gels facilitated a direct comparison of the effects of different biomechanical constraints on collagen alignment under the same biochemical culturing conditions. This reduced the complexity of our data interpretation because many cytokines and growth factors have been shown to play a role in tissue remodeling.[46,47] Indeed, effects of altered concentrations of connective tissue growth factor and transforming growth factor-beta (e.g., TGF-β1) as well as lysophosphatidic acid should be considered in future studies of altered multiaxial mechanical

loading on collagen organization. In other words, identifying optimal chemomechanical environments for tissue engineering remains of high importance.

Despite most soft tissues experiencing multiaxial loads *in vivo* (e.g., arteries, cornea, lung parenchyma, myocardium, pericardium, skin, and so forth), most tissue culture studies have focused on uniaxial loading or uniaxial constraints. It appears that Knezevic *et al.*[48] were the first to study biaxially loaded collagen gels. Thomopoulos *et al.*[16,42] subsequently used this biaxial culture system to study the development of structural and mechanical anisotropy in planar gels over 3 days. Similar to findings herein, they reported that equibiaxial loading induced little structural or mechanical anisotropy (i.e., originally isotropically oriented fibers remained so), whereas uniaxial stretching induced marked realignment of fibers toward the direction of stretch. Yet, their measured collagen fiber orientations could not explain the mechanical anisotropy that developed under uniaxial stretch.[42] Our sequential measurements of collagen fiber alignment under stretched, unloaded, and cell-free conditions provide an explanation not considered previously. Their measurements of collagen fiber orientation were performed with confocal reflectance after gel fixation in the unloaded condition, which may have been subject to some randomization by cell traction as suggested by our results.

As noted in Humphrey *et al.*,[25] two methods have proven particularly useful in biaxial mechanical testing of planar soft tissues: the use of arrays of sutures to couple square samples to the testing device, and the use of end-clamps to couple cruciform samples to the device. Although neither experimental configuration is perfect, practical issues of introducing multiple sutures into very soft collagen gels (at day 0) suggest the potential utility of cruciform samples wherein ends can be secured well for loading. Waldman and Lee[49] showed in native pericardium, for example, that mechanical properties can be estimated consistently using cruciform-shaped samples wherein the arms are 50–100% of the length of the CT region, but samples with arms only 5% of the length of the CT region result in an overly constrained material with an artificially high stiffness. Whereas Thomopoulos *et al.* used biaxial specimens with very short arms,[16,42] our cruciform specimens had arms 200% of the length of the CT region. Nevertheless, Waldman and Lee[49] further cautioned, "The sample arms underwent large deformations whereas a CT region, defined by the principal fibre directions, tended to rotate toward the direction of stretch rather than to deform." Complete characterization of biaxial culture and testing of cruciform samples should thus include in the future measurements of local strains/rotations as well as applied forces, which may need to be analyzed using finite element methods (e.g., Nielsen *et al.*[50]). Our focus herein, however, was on direct measurements of collagen fiber alignment initiated by boundary conditions commonly imposed in tissue engineering.

Significant advances in simultaneous mechanical loading, imaging, and biomechanical testing of collagen gels were achieved by Tower *et al.*,[21] who used quantitative polarized light microscopy, and Voytik-Harbin *et al.*,[14] who used confocal reflection microscopy, yet both were implemented in uniaxial cases. Another commonly used imaging method is SALS, but this method generally requires optical clearing that affects both the collagen structure and overall properties.[22,51] Moreover, like polarized light microscopy, SALS gives mean values through the thickness. Whereas biaxially loaded samples were fixed before confocal imaging in Thomopoulos *et al.*[16,42] and Lee *et al.*,[17] which did not allow the same sample to be compared across multiple states of mechanical loading or cell activity and can introduce fixation artifacts, the current NLOM-based system allowed successive intravital measurements on the same samples. Figures 2–4 reveal, for example, that comparing fiber alignment before and after mechanical loading as well as before and after lysing the cells enables one to determine (similar to Marenzana *et al.*[35] based on forces) relative effects and reversibility of stretching and cell tractions.

Conclusion

In summary, Humphrey *et al.*[25] recently showed potential advantages of combining biaxial tissue culture and opticomechanical testing. Biaxial testing allows one to compare effects of stress in the absence of strain and strain in the absence of stress as well as multiple combinations of multiaxial stress and strain. In this paper, we reported a novel biaxial culture system sufficient for such testing and suggested that cruciform-shaped samples with LAs provide a practical method for studying multiple mechanical loading states within the same gel. Moreover, SHG in NLOM can provide an excellent means for quantifying changes in collagen fiber organization within individual samples under multiple multiaxial loading conditions or states of cell activity. As illustrative results, this study demonstrated the importance of biaxial loading in the development of tissue microstructure and the potential use of diverse loads to design different tissue microstructure—static uniaxial stretch resulted in increasing collagen alignment with culture time, whereas static biaxial stretch was found to prescribe tissue anisotropy with higher fidelity. Sequential NLOM measurements of collagen fiber orientation distributions of gels stretched, unloaded, and with cells removed can also be used to delineate contributions of applied stretch, cell-mediated traction fields, and matrix remodeling on measured collagen distributions. There is, therefore, great potential to explore further the effects of multiaxial loading on cell-mediated collagen organization, information that is fundamental for increasing our understanding of native tissue mechanics as well as our ability to engineer functional tissue equivalents.

Acknowledgments

This research was supported, in part, by Grant EB-008366 from the National Institutes of Health, and NSF Faculty Early Career Development (CAREER) Award (to A.T.Y.). We thank Professor Laura Niklason at Yale University for thoughtful discussions and Kerry McLeroy for technical assistance in building the biaxial device. Equipment lists, schematics, and software of the NLOM system are available upon request. Please see http://biomed.tamu.edu/tml.

Disclosure Statement

No competing financial interests exist.

References

1. Bell, E., Ivarsson, B., and Merrill, C. Production of a tissue-like structure by contraction of collagen lattices by human fibroblasts of different proliferative potential *in vitro*. Proc Natl Acad Sci USA **76,** 1274, 1979.
2. Harris, A.K., Stopak, D., and Wild, P. Fibroblast traction as a mechanism for collagen morphogenesis. Nature **290,** 249, 1981.
3. Ehrlich, H.P. Wound closure: evidence of cooperation between fibroblasts and collagen matrix. Eye **2 (Pt 2),** 149, 1988.
4. Shi, Y., and Vesely, I. Fabrication of mitral valve chordae by directed collagen gel shrinkage. Tissue Eng **9,** 1233, 2003.
5. Grenier, G., Remy-Zolghadri, M., Larouche, D., Gauvin, R., Baker, K., Bergeron, F., Dupuis, D., Langelier, E., Rancourt, D., Auger, F.A., and Germain, L. Tissue reorganization in response to mechanical load increases functionality. Tissue Eng **11,** 90, 2005.
6. Feng, Z., Tateishi, Y., Nomura, Y., Kitajima, T., and Nakamura, T. Construction of fibroblast-collagen gels with orientated fibrils induced by static or dynamic stress: toward the fabrication of small tendon grafts. J Artif Organs **9,** 220, 2006.
7. Delvoye, P., Wiliquet, P., Leveque, J.L., Nusgens, B.V., and Lapiere, C.M. Measurement of mechanical forces generated by skin fibroblasts embedded in a three-dimensional collagen gel. J Invest Dermatol **97,** 898, 1991.
8. Brown, R.A., Prajapati, R., McGrouther, D.A., Yannas, I.V., and Eastwood, M. Tensional homeostasis in dermal fibroblasts: mechanical responses to mechanical loading in three-dimensional substrates. J Cell Physiol **175,** 323, 1998.
9. Freyman, T.M., Yannas, I.V., Yokoo, R., and Gibson, L.J. Fibroblast contractile force is independent of the stiffness which resists the contraction. Exp Cell Res **272,** 153, 2002.
10. Tomasek, J.J., Gabbiani, G., Hinz, B., Chaponnier, C., and Brown, R.A. Myofibroblasts and mechano-regulation of connective tissue remodelling. Nat Rev Mol Cell Biol **3,** 349, 2002.
11. Grinnell, F. Fibroblast biology in three-dimensional collagen matrices. Trends Cell Biol **13,** 264, 2003.
12. Roeder, B.A., Kokini, K., Sturgis, J.E., Robinson, J.P., and Voytik-Harbin, S.L. Tensile mechanical properties of three-dimensional type I collagen extracellular matrices with varied microstructure. J Biomech Eng **124,** 214, 2002.
13. Raub, C.B., Unruh, J., Suresh, V., Krasieva, T., Lindmo, T., Gratton, E., Tromberg, B.J., and George, S.C. Image correlation spectroscopy of multiphoton images correlates with collagen mechanical properties. Biophys J **94,** 2361, 2008.
14. Voytik-Harbin, S.L., Roeder, B.A., Sturgis, J.E., Kokini, K., and Robinson, J.P. Simultaneous mechanical loading and confocal reflection microscopy for three-dimensional microbiomechanical analysis of biomaterials and tissue constructs. Microsc Microanal **9,** 74, 2003.
15. Pizzo, A.M., Kokini, K., Vaughn, L.C., Waisner, B.Z., and Voytik-Harbin, S.L. Extracellular matrix (ECM) microstructural composition regulates local cell-ECM biomechanics and fundamental fibroblast behavior: a multidimensional perspective. J Appl Physiol **98,** 1909, 2005.
16. Thomopoulos, S., Fomovsky, G.M., and Holmes, J.W. The development of structural and mechanical anisotropy in fibroblast populated collagen gels. J Biomech Eng **127,** 742, 2005.
17. Lee, E.J., Holmes, J.W., and Costa, K.D. Remodeling of engineered tissue anisotropy in response to altered loading conditions. Ann Biomed Eng **36,** 1322, 2008.
18. Sacks, M.S., and Chuong, C.J. Characterization of collagen fiber architecture in the canine diaphragmatic central tendon. J Biomech Eng **114,** 183, 1992.
19. Billiar, K.L., and Sacks, M.S. A method to quantify the fiber kinematics of planar tissues under biaxial stretch. J Biomech **30,** 753, 1997.
20. Kostyuk, O., and Brown, R.A. Novel spectroscopic technique for *in situ* monitoring of collagen fibril alignment in gels. Biophys J **87,** 648, 2004.
21. Tower, T.T., Neidert, M.R., and Tranquillo, R.T. Fiber alignment imaging during mechanical testing of soft tissues. Ann Biomed Eng **30,** 1221, 2002.
22. Yeh, A.T., Choi, B., Nelson, J.S., and Tromberg, B.J. Reversible dissociation of collagen in tissues. J Invest Dermatol **121,** 1332, 2003.
23. Hirshburg, J., Choi, B., Nelson, J.S., and Yeh, A.T. Collagen solubility correlates with skin optical clearing. J Biomed Opt **11,** 040501, 2006.
24. Tan, W., Vinegoni, C., Norman, J.J., Desai, T.A., and Boppart, S.A. Imaging cellular responses to mechanical stimuli within three-dimensional tissue constructs. Microsc Res Tech **70,** 361, 2007.
25. Humphrey, J.D., Wells, P.B., Baek, S., Hu, J.J., McLeroy, K., and Yeh, A.T. A theoretically-motivated biaxial tissue culture system with intravital microscopy. Biomech Model Mechanobiol **7,** 323, 2008.
26. Larson, A.M., and Yeh, A.T. *Ex vivo* characterization of sub-10-fs pulses. Opt Lett **31,** 1681, 2006.
27. Chaudhuri, S., Nguyen, H., Rangayyan, R.M., Walsh, S., and Frank, C.B. A Fourier domain directional filtering method for analysis of collagen alignment in ligaments. IEEE Trans Biomed Eng **34,** 509, 1987.
28. Nishimura, T., and Ansell, M.P. Fast Fourier transform and filtered image analyses of fiber orientation in OSB. Wood Sci Technol **36,** 287, 2002.
29. Ng, C.P., and Swartz, M.A. Mechanisms of interstitial flow-induced remodeling of fibroblast-collagen cultures. Ann Biomed Eng **34,** 446, 2006.
30. Grinnell, F., Ho, C.H., Tamariz, E., Lee, D.J., and Skuta, G. Dendritic fibroblasts in three-dimensional collagen matrices. Mol Biol Cell **14,** 384, 2003.
31. Costa, K.D., Lee, E.J., and Holmes, J.W. Creating alignment and anisotropy in engineered heart tissue: role of boundary conditions in a model three-dimensional culture system. Tissue Eng **9,** 567, 2003.
32. Nakatsuji, N., and Johnson, K.E. Experimental manipulation of a contact guidance system in amphibian gastrulation by mechanical tension. Nature **307,** 453, 1984.
33. Guido, S., and Tranquillo, R.T. A methodology for the systematic and quantitative study of cell contact guidance in oriented collagen gels. Correlation of fibroblast orientation and gel birefringence. J Cell Sci **105 (Pt 2),** 317, 1993.
34. Wang, J.H., Jia, F., Gilbert, T.W., and Woo, S.L. Cell orientation determines the alignment of cell-produced collagenous matrix. J Biomech **36,** 97, 2003.
35. Marenzana, M., Wilson-Jones, N., Mudera, V., and Brown, R.A. The origins and regulation of tissue tension: identification of collagen tension-fixation process *in vitro*. Exp Cell Res **312,** 423, 2006.
36. Sawhney, R.K., and Howard, J. Slow local movements of collagen fibers by fibroblasts drive the rapid global self-organization of collagen gels. J Cell Biol **157,** 1083, 2002.
37. Dahlmann-Noor, A.H., Martin-Martin, B., Eastwood, M., Khaw, P.T., and Bailly, M. Dynamic protrusive cell behaviour

generates force and drives early matrix contraction by fibroblasts. Exp Cell Res **313,** 4158, 2007.
38. Feng, Z., Ishibashi, M., Nomura, Y., Kitajima, T., and Nakamura, T. Constraint stress, microstructural characteristics, and enhanced mechanical properties of a special fibroblast-embedded collagen construct. Artif Organs **30,** 870, 2006.
39. Yamato, M., Adachi, E., Yamamoto, K., and Hayashi, T. Condensation of collagen fibrils to the direct vicinity of fibroblasts as a cause of gel contraction. J Biochem **117,** 940, 1995.
40. Kessler, D., Dethlefsen, S., Haase, I., Plomann, M., Hirche, F., Krieg, T., and Eckes, B. Fibroblasts in mechanically stressed collagen lattices assume a "synthetic" phenotype. J Biol Chem **276,** 36575, 2001.
41. Nirmalanandhan, V.S., Levy, M.S., Huth, A.J., and Butler, D.L. Effects of cell seeding density and collagen concentration on contraction kinetics of mesenchymal stem cell-seeded collagen constructs. Tissue Eng **12,** 1865, 2006.
42. Thomopoulos, S., Fomovsky, G.M., Chandran, P.L., and Holmes, J.W. Collagen fiber alignment does not explain mechanical anisotropy in fibroblast populated collagen gels. J Biomech Eng **129,** 642, 2007.
43. Ehrlich, H.P., Griswold, T.R., and Rajaratnam, J.B. Studies on vascular smooth muscle cells and dermal fibroblasts in collagen matrices. Effects of heparin. Exp Cell Res **164,** 154, 1986.
44. Gillery, P., Maquart, F.X., and Borel, J.P. Fibronectin dependence of the contraction of collagen lattices by human skin fibroblasts. Exp Cell Res **167,** 29, 1986.
45. Montesano, R., and Orci, L. Transforming growth factor beta stimulates collagen-matrix contraction by fibroblasts: implications for wound healing. Proc Natl Acad Sci USA **85,** 4894, 1988.
46. Mauviel, A. Cytokine regulation of metalloproteinase gene expression. J Cell Biochem **53,** 288, 1993.
47. Bennett, N.T., and Schultz, G.S. Growth factors and wound healing: Part II. Role in normal and chronic wound healing. Am J Surg **166,** 74, 1993.
48. Knezevic, V., Sim, A.J., Borg, T.K., and Holmes, J.W. Isotonic biaxial loading of fibroblast-populated collagen gels: a versatile, low-cost system for the study of mechanobiology. Biomech Model Mechanobiol **1,** 59, 2002.
49. Waldman, S.D., and Lee, J.M. Effect of sample geometry on the apparent biaxial mechanical behaviour of planar connective tissues. Biomaterials **26,** 7504, 2005.
50. Nielsen, P.M., Hunter, P.J., and Smaill, B.H. Biaxial testing of membrane biomaterials: testing equipment and procedures. J Biomech Eng **113,** 295, 1991.
51. Wells, P.B., Yeh, A.T., and Humphrey, J.D. Influence of glycerol on the mechanical reversibility and thermal damage susceptibility of collagenous tissues. IEEE Trans Biomed Eng **53,** 747, 2006.

Address correspondence to:
Alvin T. Yeh, Ph.D.
Department of Biomedical Engineering
Texas A&M University
337 Zachry Engineering Center
3120 TAMU
College Station, TX 77843

E-mail: ayeh@tamu.edu

Received: May 16, 2008
Accepted: October 7, 2008
Online Publication Date: December 8, 2008

This article has been cited by:

1. Jin-Jia Hu, Yen-Ching Liu, Guan-Wen Chen, Mei-Xuan Wang, Pei-Yuan Lee. 2013. Development of fibroblast-seeded collagen gels under planar biaxial mechanical constraints: a biomechanical study. *Biomechanics and Modeling in Mechanobiology* **12**:5, 849-868. [CrossRef]
2. Stephen MatcherSecond-Harmonic Generation 61-92. [CrossRef]
3. M. Vielreicher, S. Schurmann, R. Detsch, M. A. Schmidt, A. Buttgereit, A. Boccaccini, O. Friedrich. 2013. Taking a deep look: modern microscopy technologies to optimize the design and functionality of biocompatible scaffolds for tissue engineering in regenerative medicine. *Journal of The Royal Society Interface* **10**:86, 20130263-20130263. [CrossRef]
4. P.-F. Lee, Y. Bai, R.L. Smith, K.J. Bayless, A.T. Yeh. 2013. Angiogenic responses are enhanced in mechanically and microscopically characterized, microbial transglutaminase crosslinked collagen matrices with increased stiffness. *Acta Biomaterialia* **9**:7, 7178-7190. [CrossRef]
5. Nicky Jonge, Frans M. W. Kanters, Frank P. T. Baaijens, Carlijn V. C. Bouten. 2013. Strain-induced Collagen Organization at the Micro-level in Fibrin-based Engineered Tissue Constructs. *Annals of Biomedical Engineering* **41**:4, 763-774. [CrossRef]
6. Elissa K. Leonard, Vincent H. Pai, Philip Amberg, Jens Gardner, Elizabeth J. Orwin. 2012. Design and validation of a corneal bioreactor. *Biotechnology and Bioengineering* **109**:12, 3189-3198. [CrossRef]
7. Jasper Foolen, Vikram S. Deshpande, Frans M.W. Kanters, Frank P.T. Baaijens. 2012. The influence of matrix integrity on stress-fiber remodeling in 3D. *Biomaterials* **33**:30, 7508-7518. [CrossRef]
8. D.D. Simon, C.O. Horgan, J.D. Humphrey. 2012. Mechanical restrictions on biological responses by adherent cells within collagen gels. *Journal of the Mechanical Behavior of Biomedical Materials* **14**, 216-226. [CrossRef]
9. Spencer P. Lake, Victor H. Barocas. 2012. Mechanics and kinematics of soft tissue under indentation are determined by the degree of initial collagen fiber alignment. *Journal of the Mechanical Behavior of Biomedical Materials* **13**, 25-35. [CrossRef]
10. Jin-Jia Hu, Wei-Chih Chao, Pei-Yuan Lee, Chih-Hao Huang. 2012. Construction and characterization of an electrospun tubular scaffold for small-diameter tissue-engineered vascular grafts: A scaffold membrane approach. *Journal of the Mechanical Behavior of Biomedical Materials* **13**, 140-155. [CrossRef]
11. B.J. Bell, E. Nauman, S.L. Voytik-Harbin. 2012. Multiscale Strain Analysis of Tissue Equivalents Using a Custom-Designed Biaxial Testing Device. *Biophysical Journal* **102**:6, 1303-1312. [CrossRef]
12. Jonathan A. Kluge, Gary G. Leisk, Robyn D. Cardwell, Alexander P. Fernandes, Michael House, Andrew Ward, A. Luis Dorfmann, David L. Kaplan. 2011. Bioreactor System Using Noninvasive Imaging and Mechanical Stretch for Biomaterial Screening. *Annals of Biomedical Engineering* **39**:5, 1390-1402. [CrossRef]
13. Joseph T. Keyes, Stacy M. Borowicz, Jacob H. Rader, Urs Utzinger, Mohamad Azhar, Jonathan P. Vande Geest. 2011. Design and Demonstration of a Microbiaxial Optomechanical Device for Multiscale Characterization of Soft Biological Tissues with Two-Photon Microscopy. *Microscopy and Microanalysis* **17**:02, 167-175. [CrossRef]
14. Jonathan Vande Geest, Joseph T. Keyes, Darren G. Haskett, Urs Utzinger, Mohamad Azhar, Jonathan Vandegeest. 2011. Adaptation of a Planar Microbiaxial Optomechanical Device for the Tubular Biaxial Microstructural and Macroscopic Characterization of Small Vascular Tissues. *Journal of Biomechanical Engineering* . [CrossRef]
15. L. E. Niklason, A. T. Yeh, E. A. Calle, Y. Bai, A. Valentin, J. D. Humphrey. 2010. Regenerative Medicine Special Feature: Enabling tools for engineering collagenous tissues integrating bioreactors, intravital imaging, and biomechanical modeling. *Proceedings of the National Academy of Sciences* **107**:8, 3335-3339. [CrossRef]